RESEARCH ARTICLE | JUNE 06 2023

Raman scattering spectra of boron imidazolate frameworks containing different magnetic ions *⊙*

Jackson Davis 💿 ; Soumyodip Banerjee; Pilar Beccar-Varela 💿 ; V. Sara Thoi 💿 ; Natalia Drichko 🗷 💿



J. Chem. Phys. 158, 214707 (2023) https://doi.org/10.1063/5.0152070





CrossMark

Articles You May Be Interested In

Beam-gas study of bismuth–fluorine reactions using laser-induced fluorescence of BiF

J. Chem. Phys. (July 1992)

Vibrational relaxation and electronic quenching rate coefficients for BiF(A0+,v') by SF 6

J. Chem. Phys. (October 1988)

Threshold oscillation of an NF($a^{1}\Delta$)/BiF visible wavelength chemical laser

Journal of Applied Physics (August 1993)

500 kHz or 8.5 GHz? And all the ranges in between.

Lock-in Amplifiers for your periodic signal measurement









Raman scattering spectra of boron imidazolate frameworks containing different magnetic ions

Cite as: J. Chem. Phys. 158, 214707 (2023); doi: 10.1063/5.0152070

Submitted: 27 March 2023 · Accepted: 19 May 2023 ·

Published Online: 6 June 2023









Jackson Davis, Doumyodip Banerjee, Pilar Beccar-Varela, Dv. Sara Thoi, Jackson Davis, David Banerjee, Dilar Beccar-Varela, Dv. Sara Thoi, Jackson Davis, David Banerjee, Dilar Beccar-Varela, Dv. Sara Thoi, Jackson Davis, David Banerjee, Dilar Beccar-Varela, Dv. Sara Thoi, Jackson Davis, Dv. Sara Thoi, Dv.











AFFILIATIONS

- Department of Physics and Astronomy, Johns Hopkins University, Baltimore, Maryland 21218, USA
- ²Department of Chemistry, Johns Hopkins University, Baltimore, Maryland 21218, USA
- Department of Materials Science and Engineering, Johns Hopkins University, Baltimore, Maryland 21218, USA
- a) Author to whom correspondence should be addressed: drichko@jhu.edu

ABSTRACT

We present a Raman scattering spectroscopic study of boron imidazolate metal-organic frameworks (BIFs) with three different magnetic metal ions and one non-magnetic in a wide frequency range from 25 to 1700 cm⁻¹, which covers local vibrations of the imidazolate linkers as well as collective lattice vibrations. We show that the spectral region above 800 cm⁻¹ belongs to the local vibrations of the linkers, which have the same frequencies for the studied BIFs without any dependence on the structure of the BIFs and are easily interpreted based on the spectra of imidazolate linkers. In contrast, collective lattice vibrations, observed below 100 cm⁻¹, show a distinction between cage and two-dimensional BIFs structures, with a weak dependence on the metal node. We identify the range of vibrations around 200 cm⁻¹, which are distinct for each metal-organic framework, depending on a metal node. Our work demonstrates the energy hierarchy in the vibrational

Published under an exclusive license by AIP Publishing. https://doi.org/10.1063/5.0152070

I. INTRODUCTION

Much of the study of metal-organic frameworks (MOFs) in recent years has focused on their tunability and porosity.1 Since MOF structures can include magnetic ions or clusters connected by organic linkers, the possibility of achieving interesting magnetic states in MOFs has been discussed.^{2,3} However, most of the recent studies of magnetic properties in MOFs have been limited by basic magnetization and magnetic susceptibility measurements. In order to study magnetism in these materials, we will need to employ spectroscopy, such as magnetic Raman scattering. In fact, magnetic Raman scattering has demonstrated its ability to probe the spectrum of magnetic excitations in organic magnetic materials^{4,5} where magnetic neutron scattering is challenging due to weak signals and the presence of hydrogen in the materials. In order to use Raman scattering spectroscopy as a tool to study different MOF structures and their magnetic response, we need to obtain information about the energy scales of all the other excitations; we must identify what part of the acquired spectroscopic information is related to the collective lattice modes, and what part is related to the linker vibrations. Vibrational Raman scattering has been widely used as a

characterization tool for MOFs because the vibrational modes within the organic ligands, and between the ligands and the metal ions, tend to produce strong peaks in the Raman spectra.6 In this manuscript, we present our vibrational Raman scattering studies of a range of MOFs, which share the same linkers but include different transitional metal ions and show three different structures. We aim to understand the hierarchy of the energy scales we observe in the very rich spectra of MOFs and develop an efficient way to interpret the spectral features.

All MOF materials studied here belong to the class of boron imidazolate frameworks (BIFs), which consist of metal ions coordinated by a boron imidazolate $[B(C_3H_3N_2)_3]$ ligand, as shown in the inset to Fig. 1. We present Raman spectra of four different BIFs with magnetic ions Cu^{2+} (S = 1/2), Ni^{2+} (S = 1), Co^{2+} (S = 3/2), and nonmagnetic Zn²⁺ as the metal cations. These BIFs have three distinct structures: Cu-BIF and Zn-BIF each possess one of two cage-like structures,^{7,8} while Co-BIF and Ni-BIF are isostructural, possessing a layered 2D triangular lattice. The cage BIFs have topologies similar to zeolites and zeolitic imidazolate frameworks (ZIFs). In ZIFs, each metal cation bonds to one nitrogen of four different

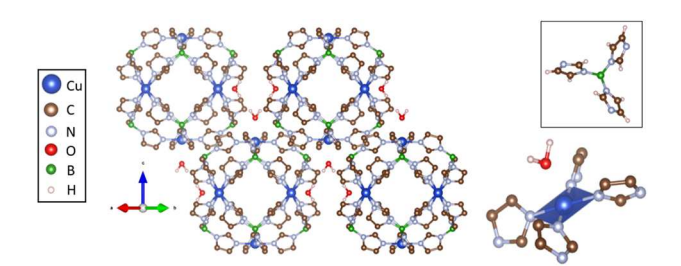


FIG. 1. Left panel: Cu–BIF cage structure. 12 Note the four-membered ring structure of the pore. Right panel: anisotropic square pyramidal Cu environment. H atoms were omitted for clarity, except those on $\rm H_2O$ that bind to Cu. Inset: boron imidazolate ligand. All structural models are visualized in VESTA. 13

imidazolate rings, creating a tetrahedral metal environment, and these linked tetrahedra form a porous 3D network of connected cages. 10 In cage BIFs, one N on the imidazolate ring binds to a metal cation, while the other binds to a $\rm B^{3+}$ cation. For instance, in the cage Cu–BIF, pictured in Fig. 1, the metal cations have an environment of four coplanar N atoms from four different imidazolate rings, while one oxygen from one $\rm H_2O$ weakly binds to the metal in the out-of-plane direction, creating a low symmetry environment for the metal atom compared to standard inorganic oxides. The Zn–BIF, pictured in Fig. 2, is composed of smaller cages of four Zn and four boron imidazolate ligands and exhibits an anisotropic tetrahedral Zn environment.

In 2D layered BIFs, no cages are formed at all, and metal ions arrange in a 2D triangular lattice (see Co octahedra in Fig. 3), which is layered along the crystallographic c axis in the bulk. In these BIFs, as illustrated for Co–BIF, metal ions are found in an octahedral environment, as the metal binds to a N atom on six imidazolate rings, as shown in Fig. 3.

The boron cations connect three of these metal-imidazolate complexes, as seen in Fig. 1. Because of this, the exchange path between metal centers passes through not only one imidazolate ring, as in ZIFs but also an extended Me-Im-B-Im-Me path, in both cage and 2D BIFs. This extended exchange path leads to a low magnetic exchange between magnetic metal centers if any at all. While the cage Cu-BIF MOF shows magnetic interactions close to zero, weak magnetic interactions have been detected in 2D layered BIFs. 11

We show that we can identify the linker vibrations that are independent of the metal ions and their environment, while the

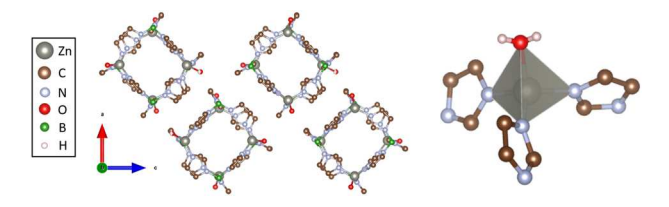


FIG. 2. Left panel: Zn-BIF cage structure. 8 Note the preserved four-membered ring structure of the pore, while the structure of the cage is different from Cu–BIF. Right panel: anisotropic tetrahedral Zn environment. H atoms were omitted for clarity, except those on H_2O that bind to Zn.

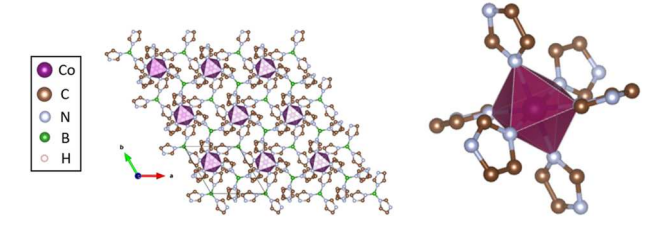


FIG. 3. Left panel: Triangular lattice structure of Co–BIF in (ab) layer.⁹ Right panel: octahedral Co environment. H atoms omitted for clarity. Ni–BIF is isostructural to Co–BIF.⁹

vibrations of the metal environment itself are sensitive to the substitution of a metal atom. Despite the differences in crystal structures, the Raman vibrations of the imidazolate linkers observed above 800 cm⁻¹ are similar for these MOFs. In contrast, the lattice vibrations observed below 100 cm⁻¹ are fingerprints of the structure. The intermediate frequencies in the range of 100–300 cm⁻¹ belong to the Raman vibrations of the metal environment and depend on the metal cation. These results demonstrate the distinct energy scales of vibrations of MOFs of different origins. This fact allows for an easy interpretation of the vibrational features of these compounds.

II. EXPERIMENTAL

MOFs were synthesized following reported literature procedures for Zn–BIF, 8 Cu–BIF, 12 and Co and Ni–BIF. 9

Raman spectra were measured using a micro-Raman option of a T64000 Horiba-Jobin-Yvon spectrometer equipped with an Olympus microscope and a LN₂ cooled CCD. Spectra were excited with the 514.5 nm line of a Coherent Innova 70C laser, with the power kept below 500 μ W for a probe of 2 μ m in diameter to avoid heating the sample. Spectra were measured at room temperature with a spectral resolution of 2 cm⁻¹ (low-energy region) and 6 cm⁻¹ (Ni, Zn, and Cu in high energy region).

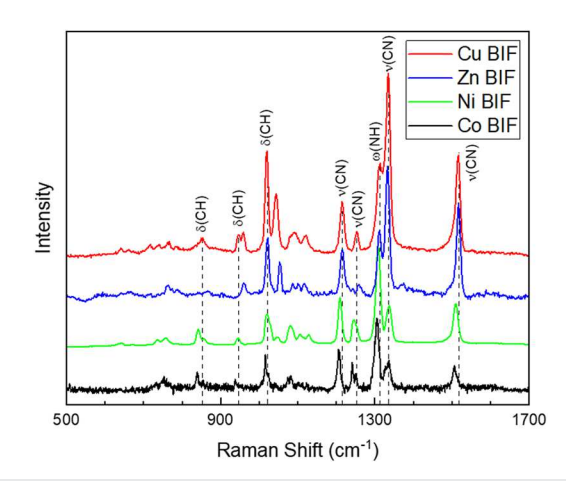


FIG. 4. Raman spectra of Cu-, Co-, Zn-, and Ni-based BIFs in the range of ligand vibrational modes. Spectra were shifted along the Y axis for clarity and normalized on the intensity of the v(CN) modes in the 1200–1250 cm⁻¹ range as stated in Sec. II

The intensity of Raman spectra for different materials was normalized on the laser power, grating reflectance, and size of the slit. To compare Raman scattering intensities of measured BIFs, vibrational spectra shown in Fig. 4 are additionally normalized to the $\nu(CN)$ modes in the 1200-1250 cm⁻¹ range; as a result, the intensity of Raman spectra $I(\omega)$ were multiplied by a constant c_1 , where $c_1 = 6.5$ for Zn-BIF, $c_1 = 16$ for Co-BIF, and $c_1 = 10$ for Cu-BIF. Similarly, low-frequency spectra were multiplied by a constant c_2 to highlight lattice modes below 100 cm⁻¹, where $c_2 = 2.5$ for Zn-BIF, $c_2 = 6.5$ for Co-BIF, and $c_2 = 10$ for Cu-BIF. Background signals of stray laser light were subtracted manually from the low-frequency Co, Cu, and Ni-BIF spectra to highlight the narrow vibrational mode peaks. A Lorentzian peak centered at 0 cm⁻¹ was used to approximately model the background to be subtracted. In Zn-BIF, a broad photoluminescent background was subtracted by comparison to the spectra of pure imidazolate containing an identical background.

III. RESULTS AND DISCUSSION

Measured Raman spectra of Co–BIF, Cu–BIF, Ni–BIF, and Zn–BIF are shown in two different regions in Figs. 4 and 5. The 500–1700 cm⁻¹ region in Fig. 4 contains the expected vibrational modes of imidazolate and allows for preliminary band assignments, which are summarized in Table I. The 0–500 cm⁻¹ region in Fig. 5 contains low-energy lattice modes below 100 cm⁻¹ and vibrational modes of metal environments above.

The Raman vibrations of imidazolate linkers are expected in the 800–1600 cm⁻¹ spectral range based on the assigned Raman spectra of ZIF-8⁶. Raman spectra of the four different BIFs have very similar frequencies of the majority of the molecular vibrations of the imidazolate ligand, despite the fact that they have three different crystal structures and four different metal nodes. This is in agreement with the expectation that the internal structure of the ligand remains unchanged between these MOFs. A comparison to previously reported Raman scattering spectra of ZIF-8⁶ reveals a direct correspondence between molecular vibrations of imidazolate in ZIF

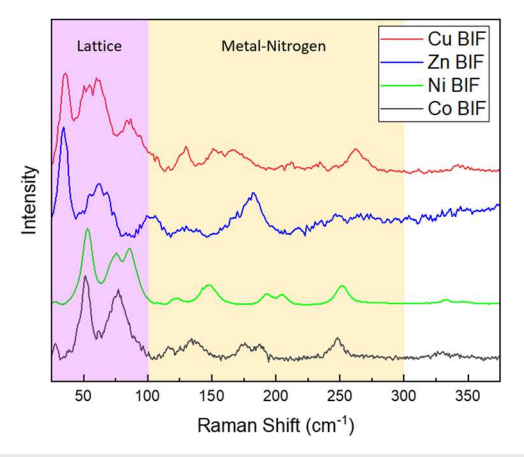


FIG. 5. Raman spectra of Cu-, Co-, Zn-, and Ni-based BIFs in the low energy region. Spectra were shifted along the Y axis and scaled by a multiplicative constant for clarity as stated in Sec. II.

TABLE I. Frequencies of Raman active vibrations of ZIF-8⁶ linkers compared to that of Co, Cu, Zn, and Ni–BIF. The assignment of the modes is based on the assignment of the Raman spectra of ZIF-8⁶. δ : bend, ν : stretch, and ω : wag. All frequencies are listed in cm⁻¹. δ (CH) are out-of-plane with respect to the imidazolate plane.

Raman mode	ZIF-8	Co-BIF	Cu-BIF	Zn-BIF	Ni-BIF
δ (CH)	834	831	853	Weak	841
δ (CH) (C4–C5)	945	939	946	960	945
δ (CH) (C2)	1023	1018	1020	1021	1021
ν(C5-N)	1143	1214	1215	1216	1210
$\nu(C-N)$	1182	1258	1252	1259	1247
ω (N–H)	1312	1316	1314	1311	1309
ν(C5-N)	1385	1343	1335	1333	1336
v(C2-N)	1507	1505	1515	1517	1510

and BIF structures and is taken as a basis for our interpretation of the vibrational spectra of BIFs. Table I summarizes the frequencies of eight molecular vibrations, which are consistent with previously reported band assignments for imidazolate ligand. We mark these assignments in the Raman spectra of the BIFs as shown in Fig. 4.

The most intense modes in the spectral region of 800–1000 cm⁻¹ are bending vibrations of C–H bonds, which are out-of-plane with respect to the plane of the imidazolate ring. These three bands are found at very similar frequencies for all measured BIFs and close to the reported frequencies in ZIF-8. The C–H bonds are the farthest away from the metals, so one would expect that their frequencies are not strongly dependent on the metal nodes.

The spectral range between 1000 and 1500 cm⁻¹ contains four stretching vibrations of C–N bonds as well as a wagging vibration of N–H. Although the positions of the two lowest bands are shifted by 70 cm⁻¹ to higher frequencies compared with the ZIF-8 spectra, the spacing of 40 cm⁻¹ between them and their relative intensities are consistent with reported ZIF spectra. The C–N stretching vibration in the range from 1334 to 1343 cm⁻¹ displays a shift to lower frequencies of 50 cm⁻¹. These differences between ZIF and BIF C–N vibrations can be attributed to the fact that the two N on an imidazolate ring bind to one metal ion and one B rather than two Zn ions as in ZIFs. Hence, the molecular vibrations that involve the N are expected to differ qualitatively between ZIF and BIF spectra, although not between BIFs themselves. In contrast, other molecular vibrations (such as C–H bending) display more consistency between ZIF and BIF spectra due to their relative isolation from the environment external to the imidazolate ring.

The reported bending vibration of the methyl group in ZIF-8⁶ is absent in BIF spectra since the imidazolate rings in the BIFs have no capping methyl group. The total suppression of the strong imidazolate ring breathing mode, found at 683 cm⁻¹ in ZIF-8, can be a result of the lower symmetry (the absence of mirror symmetry) in the linker in BIF structures, which comes from imidazolate binding to one B and one metal ion rather than two metal ions as in ZIFs. Alternatively, the suppression of this mode could be a result of a reduction of electronic density on the imidazolate ring.

The spectral range of 100–300 cm⁻¹, shown in Fig. 5, is the region of metal-ligand vibrations. The frequencies of these vibrations should be dependent both on the metal and on its coordination.¹⁴ In particular, literature data suggest stretching vibrations

TABLE II. Frequencies for four metal-N vibrational modes in the 100–300 cm⁻¹ region. Zn–BIF is not included due to the lack of four clear modes in this region. All frequencies are given in cm⁻¹.

Co-BIF	Cu-BIF	Ni-BIF	
136	129		
175	151	193	
188	169	205	
248	263	252	

TABLE III. Frequencies of observed modes below 100 cm⁻¹ for the four BIFs, presented alongside DFT-calculated THz modes of ZIF-8 with similar frequencies. ¹⁵

ZIF-8 DFT (cm ⁻¹)	Zn-BIF	Cu-BIF	Co-BIF	Ni-BIF
Ring gate opening (33)	34	35		
			52	53
Ring shearing (65)	62	58		
			77	74

of Cu-N in the octahedral environment at $280\text{--}290~\text{cm}^{-1}$ and Zn in a tetrahedral environment at 207 cm⁻¹. ¹⁴ Modes in this region, therefore, belong to the stretching N-metal vibration. In the molecular approximation, the number of modes would depend on the number of atoms in the environment, which explains the lower number of vibrations observed for the tetrahedral metal environment in Zn-BIF compared to the octahedral environments of metals in the other studied BIFs. Zn-BIF has one mode at 181 cm⁻¹, while Co, Cu, and Ni have four weak modes at frequencies summarized in Table II. The similarity between Ni and Co-BIF N-metal vibrations is consistent with the identical octahedral environments of Ni and Co, with the small shift in frequencies potentially arising from a change in electronic density on the N atoms in the metal environment. The more significant differences in this region in the Cu and Zn-BIF spectra are consistent with their unique metal environments.

Figure 5 also presents the low frequency spectra of the BIF MOFs. Typically for molecular crystals, the region below 100 cm⁻¹ corresponds to lattice vibrations, which would depend on the structure of the MOFs. While to the best of our knowledge, there is no spectroscopic information on the lattice modes of BIFs, and the lattice "collective" modes of ZIFs were studied to some extent by THz spectroscopy, neutron scattering, and density functional theory (DFT) calculations and were also found below 100 cm⁻¹ t5,16

In our experimental data, we find that two low-frequency vibrations of the cage Cu and Zn–BIFs occur at similar frequencies, while 2D Ni and Co–BIFs have similar low-frequency spectra, distinct from the cage BIFs (see Table III). This demonstrates a distinct dependence of the lattice mode spectra on the structure of the MOFs, showing that the lattice vibrations are fingerprints of a particular lattice structure and not the chemical environment. We find that two of the lattice modes observed in the spectra for the two cage BIFs, Cu and Zn, are similar to Raman-active THz modes in the calculated DFT spectra of ZIF-8, which is also composed of a porous cage-like

structure. These include a strong mode at 33 cm⁻¹, which is assigned to a symmetric four-membered ring (see Figs. 1 and 2) gate opening, and a mode at 65 cm⁻¹, which is assigned to a four-membered ring shearing.¹⁵

The 2D layered BIFs, on the other hand, do not display any similarity to calculated THz modes of ZIFs, which is consistent with the significant structural differences between the 2D triangular lattice structure and the various cage structures. DFT calculations on the 2D structures are necessary to further interpret these vibrations.

IV. CONCLUSIONS

In this work, we have presented Raman scattering spectra of BIF MOFs with different metal ions in a frequency range between 30 and 2000 cm⁻¹ and demonstrated a separation between the energy scales related to the different types of vibrations of the MOFs. The high frequency region of the spectra above 500 cm⁻¹ contains Raman-active vibrational modes of imidazolate ligands, which are similar between four different BIFs with different structures and metal nodes. They can be assigned based on the literature data of MOFs with the same linker molecules, ZIFs.

The low-energy region of the spectra below 100 cm⁻¹ demonstrates consistency in lattice modes of isostructural BIFs. The modes of the cage BIFs have frequencies similar to the calculated lattice modes for ZIFs, while 2D BIFs have a distinctly different lattice mode spectrum. These results demonstrate that the lattice vibrations of MOFs are fingerprints of a certain structure.

The spectral region between $\sim \! 100$ and $300~\rm cm^{-1}$ is dominated by the vibrations of the metal environment. The frequencies of vibrations observed in this region depend on the metal atom but show some consistency between BIFs with different metals in the same environment.

The consistency of lattice modes and ligand vibrations provides an efficient way to understand and assign the spectra of MOFs without performing full calculations of the vibrational response of each MOF structure.

SUPPLEMENTARY MATERIAL

We present unprocessed Raman scattering spectra of the BIFs in the supplementary material as well as the backgrounds used for the background subtraction described in Sec. II.

ACKNOWLEDGMENTS

Acknowledgment is made to the donors of the American Chemical Society Petroleum Research Fund for partial support of this research. We acknowledge the support of the NSF under Award No. DMR-2004074. S.B., P.B.-V., and V.S.T. acknowledge support by the U.S. Department of Energy (DOE), Office of Science, Office of Basic Energy Sciences, Catalysis Science program, under Award No. DE-SC0021955. P.B.-V. acknowledges the Dean's ASPIRE grant from the Office of Undergraduate Research, Scholarly and Creative Activity at Johns Hopkins University.

AUTHOR DECLARATIONS

Conflict of Interest

The authors have no conflicts to disclose.

Author Contributions

Jackson Davis: Data curation (equal); Formal analysis (equal); Investigation (equal); Writing – original draft (equal); Writing – review & editing (equal). Soumyodip Banerjee: Resources (equal). Pilar Beccar-Varela: Resources (equal). V. Sara Thoi: Resources (equal); Supervision (equal); Writing – review & editing (equal). Natalia Drichko: Conceptualization (equal); Investigation (equal); Project administration (equal); Supervision (equal); Writing – original draft (equal); Writing – review & editing (equal).

DATA AVAILABILITY

The data that support the findings of this study are available from the corresponding author upon reasonable request.

REFERENCES

- ¹M. Safaei, M. M. Foroughi, N. Ebrahimpoor, S. Jahani, A. Omidi, and M. Khatami, "A review on metal-organic frameworks: Synthesis and applications," TrAC Trends Anal. Chem. **118**, 401–425 (2019).
- ²A. E. Thorarinsdottir and T. D. Harris, "Metal-organic framework magnets," Chem. Rev. 120, 8716–8789 (2020).
- ³G. Mínguez Espallargas and E. Coronado, "Magnetic functionalities in MOFs: From the framework to the pore," Chem. Soc. Rev. 47, 533–557 (2018).
- ⁴N. Drichko, R. Hackl, and J. A. Schlueter, "Antiferromagnetic fluctuations in a quasi-two-dimensional organic superconductor detected by Raman spectroscopy," Phys. Rev. B **92**, 161112 (2015).

- ⁵N. Hassan, S. Cunningham, M. Mourigal, E. I. Zhilyaeva, S. A. Torunova, R. N. Lyubovskaya, J. A. Schlueter, and N. Drichko, "Evidence for a quantum dipole liquid state in an organic quasi-two-dimensional material," Science 360, 1101–1104 (2018).
- ⁶K. I. Hadjiivanov, D. A. Panayotov, M. Y. Mihaylov, E. Z. Ivanova, K. K. Chakarova, S. M. Andonova, and N. L. Drenchev, "Power of infrared and Raman spectroscopies to characterize metal-organic frameworks and investigate their interaction with guest molecules," Chem. Rev. 121, 1286–1424 (2021).
- ⁷D.-X. Zhang, H.-X. Zhang, H.-Y. Li, T. Wen, and J. Zhang, "Self-assembly of metal boron imidazolate cages," Cryst. Growth Des. 15, 2433–2436 (2015).
- ⁸T. Wen and J. Zhang, "Rational design of metal boron imidazolate cages to frameworks," Inorg. Chim. Acta Next Gener. **460**, 89–92 (2017).
- ⁹S. Banerjee, X. Han, M. A. Siegler, E. M. Miller, N. M. Bedford, B. C. Bukowski, and V. S. Thoi, "Flexible 2D boron imidazolate framework for polysulfide adsorption in lithium–sulfur batteries," Chem. Mater. **34**, 10451 (2022).
- ¹⁰ B. Chen, Z. Yang, Y. Zhu, and Y. Xia, "Zeolitic imidazolate framework materials: Recent progress in synthesis and applications," J. Mater. Chem. A 2, 16811–16831 (2014).
- ¹¹J. Davis *et al.*, "Tuning magnetic exchange in boron imidazolate frameworks by substitution of metal ions and lattice structure," (unpublished) (2023).
- 12 S. Banerjee, J. M. Gorham, P. Beccar-Varela, H. G. Hackbarth, M. A. Siegler, N. Drichko, J. T. Wright, N. M. Bedford, and V. S. Thoi, "Atomically dispersed CuN_{x} sites from thermal activation of boron imidazolate cages for electrocatalytic methane generation," ACS Appl. Energy Mater. (published online, 2022).
- ¹³K. Momma and F. Izumi, "VESTA 3 for three-dimensional visualization of crystal, volumetric and morphology data," J. Appl. Crystallogr. 44, 1272–1276 (2011).
- ¹⁴M. Andersson, J. Hedin, P. Johansson, J. Nordström, and M. Nydén, "Coordination of imidazoles by Cu(II) and Zn(II) as studied by NMR relaxometry, EPR, far-FTIR vibrational spectroscopy and ab initio calculations: Effect of methyl substitution," J. Phys. Chem. A **114**, 13146–13153 (2010).
- ¹⁵M. R. Ryder, B. Civalleri, T. D. Bennett, S. Henke, S. Rudić, G. Cinque, F. Fernandez-Alonso, and J.-C. Tan, "Identifying the role of terahertz vibrations in metal-organic frameworks: From gate-opening phenomenon to shear-driven structural destabilization," Phys. Rev. Lett. 113, 215502 (2014).
- ¹⁶ A. F. Méslein and J.-C. Tan, "Vibrational modes and terahertz phenomena of the large-cage zeolitic imidazolate framework-71," J. Phys. Chem. Lett. 13, 2838–2844 (2022).